Polymer 51 (2010) 1404–1412

Contents lists available at ScienceDirect

Polymer

journal homepage: www.elsevier.com/locate/polymer

A infrared spectroscopic study on the mechanism of temperature-induced phase transition of concentrated aqueous solutions of poly(N-isopropylacrylamide) and N-isopropylpropionamide

Hengjie Lai, Peiyi Wu*

The Key Laboratory of Molecular Engineering of Polymers, Ministry of Education, Department of Macromolecular Science, Laboratory of Advanced Materials, Fudan University, Shanghai 200433, PR China

ARTICLE INFO

Article history:
Received 16 November 2009
Received in revised form
12 January 2010
Accepted 17 January 2010
Available online 1 February 2010

Keywords:
Poly(N-isopropylacrylamide)
N-isopropylpropionamide
Perturbation correlation moving window

ABSTRACT

FTIR in combination with perturbation correlation moving window (PCMW) technique was applied to study the phase transition of concentrated aqueous solutions of Poly(N-isopropylacrylamide) (PNIPAM) and its small molecular model compound N-isopropylpropionamide(NIPPA). It was found that lower critical solution temperature (LSCT) of 40% NIPPA/D_2O solution was 39 °C which was higher by *ca.* 8 °C than that of PNIPAM, and that NIPPA exhibited much wider temperature ranges of phase transition from 30 to 50 °C while PNIPAM underwent the phase separation in a narrow temperature range (29.1–33.1 °C). Moreover, we utilized two-dimensional correlation infrared spectroscopy (2DIR) analysis to reveal that the presence of main chains didn't affect the sensitivity and changing sequence of different groups, but did have a strong effect on the size of aggregation and formation of hydrogen bonds between carbonyl groups and water molecules. Without the interference of hydrophobic main chains, the carbonyls of NIPPA (1600 cm^{-1}) could interact with more water than those of PNIPAM (1627 cm^{-1}) below LSCT, which was the reason of the slower and milder phase transition taking place in NIPPA system.

1. Introduction

Poly(N-isopropylacrylamide) (PNIPAM) is a well-known temperature-sensitive polymer whose aqueous solutions undergo coil–globule transition above its lower critical solution temperature (LCST) [1–3]. Several research groups have investigated the mechanism of this phase separation using various kinds of methods, including high-frequency dielectric relaxation techniques [4,5], NMR [6–8], differential scanning calorimetry [9–12], IR spectroscopy [13–18], Raman spectroscopy [19–21] and quantum chemical calculations [2,21,22].

Recently, there are two "contrary" viewpoints reported in view of the phase behavior of PNIPAM (Scheme 1(a)) and its small molecular model compound, N-isopropylpropionamide (NIPPA) (Scheme 1(b)). A dielectric relaxation study [5] revealed that the number of water molecules hydrated with NIPPA kept a constant value above the LCST of 32 °C, while the value for aqueous PNIPAM solution changed sharply at the LCST. The phase behavior of NIPPA solution in deuterated water has been investigated by Meersman et al. [23]. Different features have been illustrated clearly via temperature–composition phase diagram of NIPPA/D_2O and PNIPAM/D_2O, and FTIR spectral changes of amide groups also proved that part of NIPPA molecules took place liquid–liquid phase transition upon heating. A linear band shift in amide groups can be observed at 5 wt% NIPPA/D_2O solution in which no separation occurs. In contrast, at wt = 30%, the amide band exhibited a red shift in an "S-shaped" manner, indicating that deuterated water could get rid of amide groups during liquid–liquid phase transition. Therefore, the concentration played an important role in NIPPA system.

Perturbation correlation moving window (PCMW) is a new analytical tool, whose basic principles base on the conventional moving window proposed by Thomas and Richardson [24]. Morita et al. [25] developed this technique to expand applicability of researches by introducing the variable perturbation into correlation equation. One of the advantages of this method is that a typical point (such as LCST) of a spectral intensity variation could be visualized in the PCMW correlation spectra. Another one is that complicated spectral intensity variation along the perturbation direction can be detected. For example, Morita et al. [26] utilized the PCMW correlation analysis to find that the recrystallization of non-annealed poly(3-hydroxybutyrate) (PHB) took place between 40 and 110 °C and the melting temperature could be measured at 190 °C by the sharp change to the broad amorphous C=O stretching absorption.

Generalized two-dimensional (2D) correlation spectroscopy is another analytical technique firstly proposed by Noda [27,28],

* Corresponding author.
E-mail address: peiyiwu@fudan.edu.cn (P. Wu).

0032-3861/$ – see front matter © 2010 Elsevier Ltd. All rights reserved.
doi:10.1016/j.polymer.2010.01.036

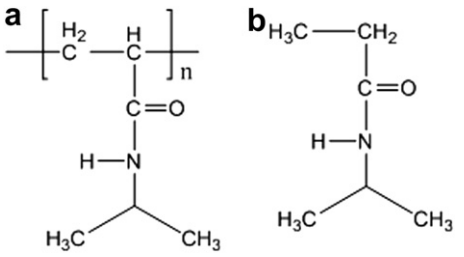

Scheme 1. Chemical structure of PNIPAM (a) and NIPPA (b).

which can be used to investigate the spectral intensity fluctuation under a specific perturbation such as temperature, time, pH or concentration etc. In a word, 2D correlation analysis can not only find out complex or overlapped spectral information and enhance spectral resolution, but also it can obtain a series of vibration sequence of special groups.

In the present study, we mainly focus on the infrared spectral changes of C–H and Amide I groups during heating process in 40% PNIPAM/D_2O and 40% NIPPA/D_2O solution. Comparing with PNIPAM system, we investigate the differences in experimental results of LCST and temperature ranges of phase separations, and provide another evidence for the phase behavior of NIPPA aqueous solution through PCMW. Moreover, we further reveal the specific event sequence of different groups in heating process by 2DIR technique, which may be helpful to understand the different phase behaviors of PNIPAM and NIPPA on a molecular level.

2. Experimental section

2.1. Material and synthesis

N-isopropylacylamide (NIPAM) monomers were purchased from Tokyo Kasei Kogyo Co. (Tokyo, Japan) and used with further purification. Poly(N-isopropylacylamide) (PNIPAM) was synthesized by free-radical polymerization in tetrahydrofuran (THF) as solvent. The reaction was initiated by azobis (isobutyronitrile) (AIBN) and carried out at 70 °C for 12 h under nitrogen atmosphere. After precipitations, products were dried under vacuum to constant weight. The molecular weight of PNIPAM, $M_w = 2498$, and polydispersity index, $M_w/M_n = 1.34$, were measured by a Voyager DE-STR matrix-assisted laser desorption/ionization time-of-flight (MALDI-TOF MS) mass spectrometer equipped with a 337 nm nitrogen laser.

N-isopropylpropionamide (NIPPA) was synthesized by the well-known Schotten–Baumann reaction. Propionyl chloride (0.1 mol) were added dropwise into isopropyl amine (0.11 mol)/Triethylamine (0.09 mol)/THF solution in the ice-water bath under continuous stirring. After removal of amine hydrochloride by filtration, the residue was shaken with 2 mol/L aqueous $NaHCO_3$, and then it were dried with anhydrous sodium sulfate. After removal of sodium sulfate, residual solvent was removed via rotary evaporation. The product was stored in a dessicator to minimise the absorption of water. The chemical structure and purity of NIPPA in deuterated chloroform was confirmed by ^1H NMR (Varian Mercury plus 400) (δ, ppm, 25 °C): 5.28 (s, 1H), 4.09 (m, 1H), 2.16 (q, 2H), 1.16 (m, 9H). The composition has been determined by element analysis (ELEMEN TAR VARIO EL3): C, 62.6; H, 11.3; N, 12.15.

2.2. Sample preparation

PNIPAM and NIPPA were respectively dissolved in deuterated water (Cambridge Isotope Laboratories, Inc., D-99.9%) with a concentration of 40 wt%. The solution was kept for two days before experiments in order to ensure the complete deuteration of all the NH-protons.

2.3. Fourier transform infrared spectroscopy

The samples of PNIPAM and NIPPA deuterated water solutions were respectively placed in the middle of two CaF_2 tablets. The FTIR spectra were measured on a Nicolet Nexus 470 spectrometer equipped with a DTGS detector. A total of 32 scans at a resolution of 4 cm^{-1} were collected. Variable-temperature spectra were controlled between 22 and 41 °C with an increment of 1 °C for 40% PNIPAM/D_2O solution as well as between 18.5 and 70.5 °C with an increment of 2 °C for 40% NIPPA/D_2O solution. The data processing was performed by the software of OMNIC 8.0.

2.4. Two-dimensional correlation analysis

Baseline correction was performed for all spectra in certain wavenumber ranges before calculation of the 2D correlation. The generalized 2D correlation analysis was applied by the 2D Shige ver. 1.3 (Shigeaki Morita, Kwansei-Gakuin University, Japan, 2004–2005) tailored by Shigeaki Morita, and was further plotted by Origin program 8.0 in order to obtain 2D correlation maps with good quality and clarity. In the 2D contour maps, the red-colored regions are defined as the positive correlation intensities, while the blue-colored ones mean the negative correlation intensities.

2.5. Perturbation correlation moving window

Perturbation correlation moving window (PCMW) is expressed as a pair of synchronous and asynchronous correlation spectra plotted on a plane between a spectral variable axis and a perturbation variable axis. FTIR spectra were carried out with this method and further correlation information was also calculated by the software 2D Shige with window size ($2m + 1 = 9$). Similarly, the contour maps were plotted by Origin program 8.0 with the same colors defined as the same means as 2D correlation analysis.

2.6. Differential scanning calorimetry

DSC measurements of the 40 wt% PNIPAM/D_2O or 40 wt% NIPPA/D_2O solutions were performed by Mettler-Toledo DSC 1 with a scanning rate of 15 °C/min. This was run with one heating scan in the −10 to 100 °C temperature range.

3. Results and discussion

3.1. DSC analysis for NIPPA and PNIPAM systems

Fig. 1 shows the DSC thermographs of 40 wt% PNIPAM/D_2O solution (a) and 40 wt% NIPPA/D_2O solution (b). As can be seen in Fig. 1(a), the sharp peak of endothermic transition is obtained around 33.5 °C for polymer system. Furthermore, we just find a small and broad peak in the NIPPA system (seen in Fig. 1(b)), and the temperature corresponding to the peak value is 37.5 °C. From above comparison, we can find that PNIPAM aqueous solution undergoes a drastic phase separation because calorimetric enthalpy of PNIPAM is much larger than that of NIPPA. In addition, it is notable that temperature range of phase transition is from 29 °C to 40 °C in PNIPAM system, while the small and asymmetric peak actually ranges from 30 to 60 °C, suggesting that cooperativity of the dehydration of NIPPA is low and that the phase transition takes place in a much slower process upon heating. In order to

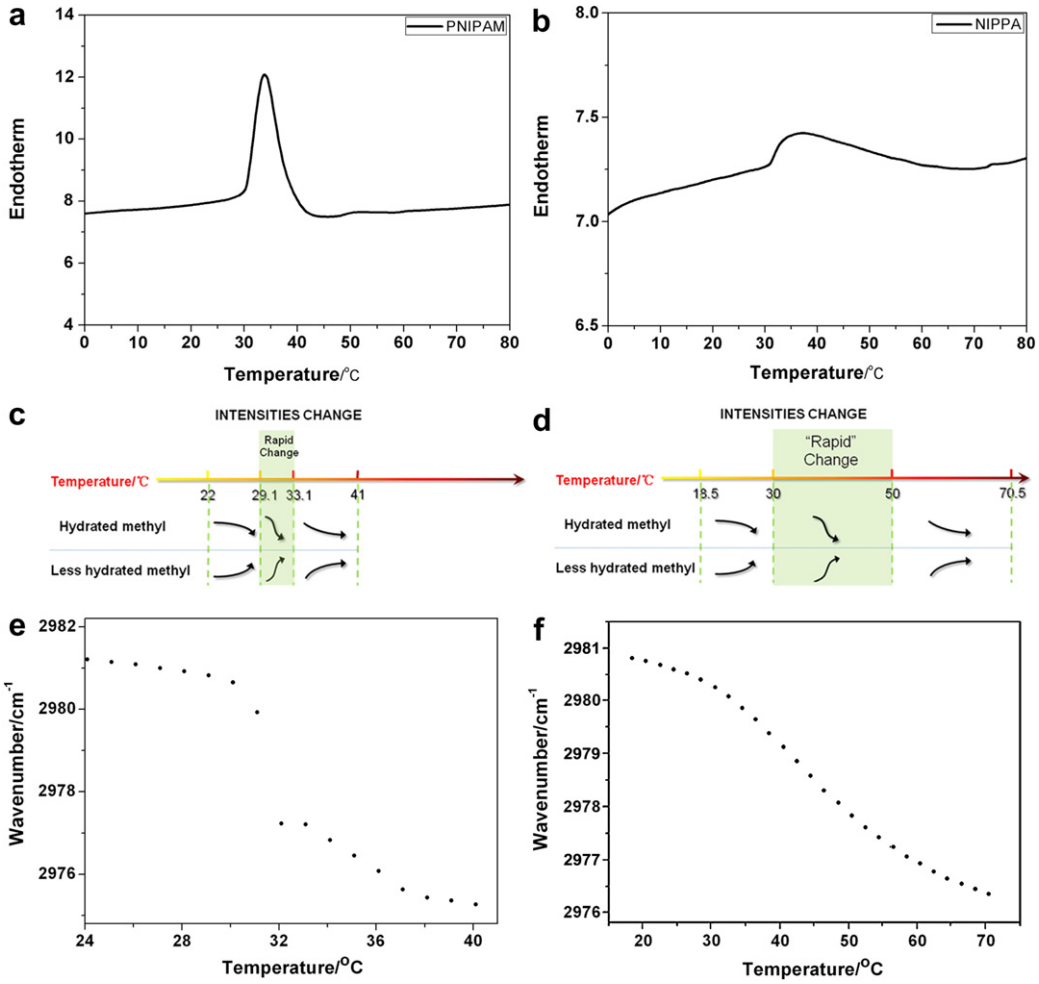

Fig. 1. Heating DSC thermograms for aqueous solution of PNIPAM (a) and NIPPA (b). Schematic diagram of intensities change of hydrated methyl and less hydrated methyl in NIPPA system (c) and PNIPAM system (d). Spectral variation in the methyl band of PNIPAM (e) and NIPPA (f) as a function of temperature. Solution concentrations of two samples: 40 wt% for PNIPAM and 40 wt% for NIPPA. * - emphasizes that the concentrations are same in two different solutions.

confirm and explain the DSC results, we further study these molecular mechanisms of phase transitions by IR, PCMW and 2DIR analysis.

3.2. IR & PCMW analysis for PNIPAM systems

The temperature-induced spectral variations in the C–H region of PNIPAM aqueous solution have been investigated by several independent research groups. According to literature, the number of hydrated $-CH_3$ groups would decrease sharply above LCST in the temperature-elevation process because the hydration interaction had been weakened.

Fig. 2 shows the temperature dependence of the absorption band of the C–H region. This region is mainly composed of three distinct peaks [29]: $\nu_{as}(CH_3)$ of the side chains of PNIPAM at *ca.* 2981 cm^{-1}, $\nu_{as}(CH_2)$ of the main chains at *ca.* 2939 cm^{-1} and $\nu_s(CH_3)$ of the side chains of PNIPAM at *ca.* 2881 cm^{-1}. Several spectral changes can be easily observed in Fig. 2, the bands of $\nu_{as}(CH_3)$, $\nu_{as}(CH_2)$ and $\nu_s(CH_3)$ all shift to the lower wavenumber upon heating. What's more, the most significant red shift happens when the temperature reaches above LCST (around 32 °C). Therefore, it truly reveals dehydration of the CH_3 and CH_2 groups is also a sign for phase transition just as hydrogen bonds of C═O···D–O–D are partially destroyed during the coil-to-globule transition.

As is mentioned before, perturbation correlation moving window is a powerful method to determine the transition point. The PCMW spectra calculated from the temperature-dependent IR spectra of the PNIPAM 40 wt% D_2O solution in the 3060–2850 cm^{-1}

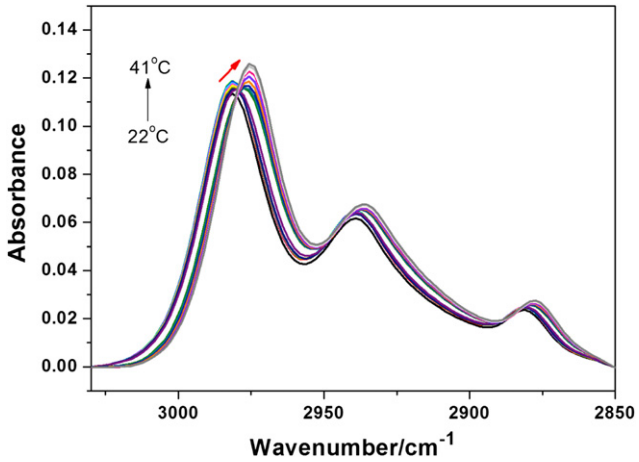

Fig. 2. FTIR spectral variations in the CH region of PNIPAM 40 wt% D_2O solution as a function of temperature. The temperature was varied between 22 and 41 °C with an interval of 1 °C.

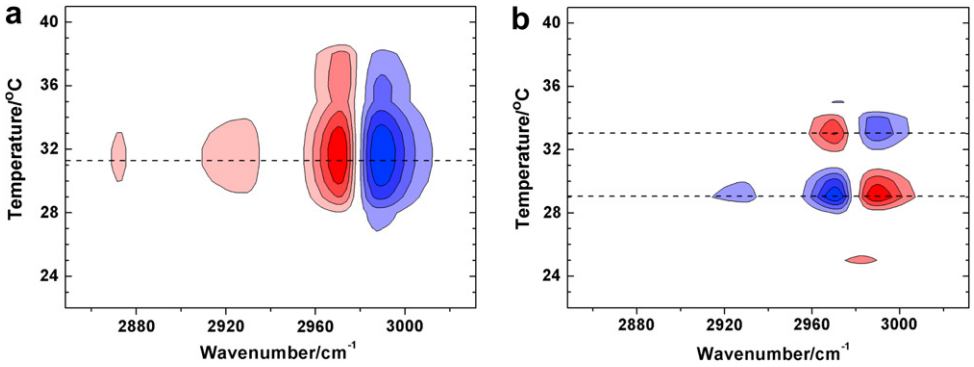

Fig. 3. 2D synchronous (a) and asynchronous (b) spectra of PCMW performed in the temperature range 22–41 °C in the regions (3060–2850 cm^{-1}) of PNIPAM 40 wt% D_2O solution. Red colors are defined as positive intensities, while blue colors as negative ones. (For interpretation of the references to colour in this figure legend, the reader is referred to the web version of this article.)

region are shown in Fig. 3. Both synchronous and asynchronous PCMW spectra are composed of a wavenumber axis and a temperature axis. In the synchronous spectrum (Fig. 3(a)), it is notable that the band of $\nu_{as}(CH_3)$ is divided into two peaks: the red one is centered at about 2970 cm^{-1} which can be attributed to the less hydrated methyl groups, and the blue one is centered at 2990 cm^{-1} which can be attributed to the hydrated methyl groups. More important, LCST (31.2 °C) and the temperature range of phase transition (29.1–33.1 °C) of PNIPAM aqueous solution could be easily found from the synchronous spectrum (Fig. 3(a)) and asynchronous spectrum (Fig. 3(b)), respectively. These results agree well with the conclusion other researchers have reported [30] and our DSC result.

According to the rule of PCMW (in the case of linear increment perturbation) summarized in Table 1 by Morita et al. [25], the synchronous PCMW correlation spectrum represents a direct correlation between the spectral intensity change and the given perturbation change, while the asynchronous one is a correlation between the spectral intensity change and a discrete Hilbert transform of the perturbation change. Therefore, positive region (red-colored region) in synchronous correlation represents spectral intensity increment, while negative one (blue-colored region) represents decrement. And positive asynchronous correlation means a convex spectral intensity variation while negative one means a concave variation. Besides, zero region (white-colored region) means linear change in both two PCMW spectra.

Table 1
Rules of PCMW correlation spectroscopy [25].

Synchronous	Asynchronous	Spectral change
+	+	Convex increment
+	0	Linear increment
+	−	Concave increment
0	+	Convex top
0	0	Constant
0	−	Concave bottom
−	+	Convex decrement
−	0	Linear decrement
−	−	Concave decrement

So negative region at 2990 cm^{-1} in Fig. 3(a) implies that deuterated water molecules leave from methyl groups and the number of hydrated methyl groups is decreasing. As a result, less hydrated methyl groups (2970 cm^{-1}) are becoming more and more. Hence, we can figure out the dehydration mainly happens to methyl groups as the PNIPAM solution undergoes phase separation at 31.2 °C upon heating.

Moreover, let us consider the correlation peaks observed in both the synchronous and asynchronous PCMW spectra. The variation in hydrated methyl band below LCST is expressed as synchronous spectra (2990 cm^{-1}, 29.1 °C) < 0 and asynchronous spectra (2990 cm^{-1}, 29.1 °C) > 0. These results suggest that the spectral intensity change should be a convex decrement according to the rule of PCMW (seen in Table 1). On the other hand, above the characteristic temperature of LCST at hydrated methyl band, synchronous spectra (2990 cm^{-1}, 33.1 °C) < 0 and asynchronous spectra (2990 cm^{-1}, 33.1 °C) < 0. It implies that spectral intensity change should be a concave decrement. Around LCST (31.2 °C), we can find synchronous spectra (2990 cm^{-1}, 31.2 °C) < 0 and asynchronous spectra (2990 cm^{-1}, 31.2 °C) $= 0$. These results demonstrate that the spectral intensity exhibits a linear decrement. Therefore, the integral intensities of all three regions appear to show an interesting image—"anti-S-shape" decrement.

For the less hydrated methyl groups that are centered at about 2970 cm^{-1}, there are also three types of intensity change: Below LCST, synchronous spectra (2970 cm^{-1}, 29.1 °C) > 0 and asynchronous spectra (2970 cm^{-1}, 29.1 °C) < 0; Above LCST, synchronous spectra (2970 cm^{-1}, 33.1 °C) > 0 and asynchronous spectra (2970 cm^{-1}, 33.1 °C) > 0; Around LCST, synchronous spectra (2970 cm^{-1}, 31.2 °C) > 0 and asynchronous spectra (2970 cm^{-1}, 31.2 °C) $= 0$. They are described as a concave increment, a convex increment and a linear increment, respectively. So this process can be depicted as "S-shape" increment which is opposite to the change of hydrated methyl groups completely (seen in Fig. 1(c)).

In a previous work, we presented that the dehydration process could be divided into two steps [14]. Methyl groups hydrated with many water molecules first changed to the less hydrated methyl groups, then less hydrated methyl groups would further dehydrated with a second step. In this paper, we find, by means of PCMW analysis, another important phenomenon that less hydrated methyl groups exists a rapid change between 29.1 and 33.1 °C during heating process. So according to dehydrated formation rate, the intensity change of hydrated methyl undergoes three-step process: Firstly, many water molecules interact with methyl groups, and only a small fraction of water gets rid of methyl groups before 29.1 °C;

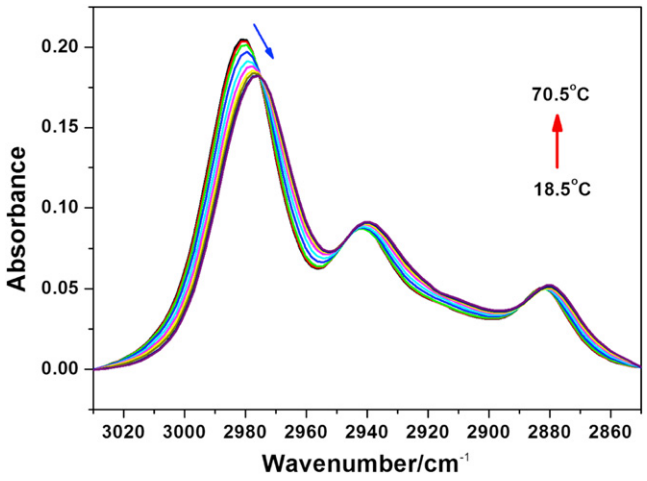

Fig. 4. FTIR spectral variations in the CH region of NIPPA 40 wt% D_2O solution as a function of temperature. The temperature was varied between 18.5 and 70.5 °C with an interval of 2 °C.

Secondly, a lot of water molecules rapidly escape from methyl groups so that the intensity of hydrated methyl groups exhibits sharp decrement between 29.1 and 33.1 °C; Thirdly, the dehydrated process of methyl groups keep stable gradually after 33.1 °C.

Among them, the second significant step represents the core of "S-shape" or "anti-S-shape" intensity change, which is also a typical sign of phase transition. Therefore, it indicates that PCMW is really a useful method to find the transition points and greatly simplify the investigation of complicated spectral variations.

3.3. IR & PCMW analysis for NIPPA systems

In Fig. 4, the change of the absorption band of $-CH_3$ groups and $-CH_2-$ groups in 40 wt% NIPPA/D_2O solution have been monitored from 18.5 to 70.5 °C. Similarly, this region is also mainly composed of three distinct peaks: $\nu_{as}(CH_3)$ at about 2979 cm^{-1}, $\nu_{as}(CH_2)$ at about 2929 cm^{-1} and $\nu_s(CH_3)$ at about 2871 cm^{-1}. From conventional IR spectra, we can find all peaks shift to the low wavenumber, especially the red shift of $\nu_{as}(CH_3)$ during heating process. And it is noteworthy that rapid shift of NIPPA aqueous solution is not as significant as one of PNIPAM aqueous solution.

Fig. 5 is the 2D synchronous and asynchronous spectra of PCMW in NIPPA system. Combining with synchronous and asynchronous spectral information of $\nu_{as}(CH_3)$ region, we can read the transition point is at about 39 °C, and that synchronous spectra (2987 cm^{-1}, 30.0 °C) < 0, asynchronous spectra (2987 cm^{-1}, 30.0 °C) > 0 below the transition point, and that synchronous spectra (2987 cm^{-1}, 50.0 °C) < 0, asynchronous spectra (2987 cm^{-1}, 50.0 °C) < 0 above the transition point, and that synchronous spectra (2987 cm^{-1}, 39 °C) < 0, asynchronous spectra (2987 cm^{-1}, 39 °C) = 0 around the transition point. It indicated that intensities change of the band at 2987 cm^{-1} assigned to hydrated methyl groups can be described as "anti-S-shape" decrement in accordance with the rules of PCMW. Additionally, another absorption bands centered at *ca.* 2966 cm^{-1} can be attributed to the vibration of less hydrated methyl groups of NIPPA molecules. In this region, there are also three steps of intensities change: synchronous spectra (2966 cm^{-1}, 30.0 °C) > 0, asynchronous spectra (2966 cm^{-1}, 30.0 °C) < 0 below the transition point, and synchronous spectra (2966 cm^{-1}, 50.0 °C) > 0, asynchronous spectra (2966 cm^{-1}, 50.0 °C) > 0 above the transition point, and synchronous spectra (2966 cm^{-1}, 39 °C) > 0, asynchronous spectra (2966 cm^{-1}, 39 °C) = 0 around the transition point. This result shows that the intensities change of less hydrated methyl are followed by the mode of "S-shape" increment which depicted in Fig. 1(c and f).

Table 2
Different features of phase behaviors in PNIPAM and NIPPA.

Systems	LSCT/°C	Temperature ranges of phase transition/°C	State of phase transition
40% PNIPAM/D_2O	31.2	29.1–33.1	Liquid → solid
40% NIPPA/D_2O	39	30–50	Liquid → liquid

Comparing with the spectral conclusion of phase transition in PNIPAM/D_2O solution, we can find several similar points. Firstly, methyl groups are divided into two different conformations including hydrated methyl and less hydrated methyl in both systems. It is well known that dehydration processes can both take place during heating in PNIPAM/D_2O solution and NIPPA/D_2O solution. Secondly, the whole intensities change of methyl groups is not linear but "anti-S-shape" or "S-shape", which is a striking feature to manifest some kind of temperature-induce phase transition exists in two systems.

Except for these two similar results, there are some distinct features listed in Table 2. Most of all, the former phase transition is the conformation change of liquid and solid phases, while the other one is called liquid–liquid separation. Secondly, the rapid change takes place between 30 and 50 °C in NIPPA/D_2O solution in comparison with the PNIPAM system which have narrow temperature range (from 29.1 to 33.1 °C) when the rapid change happens.

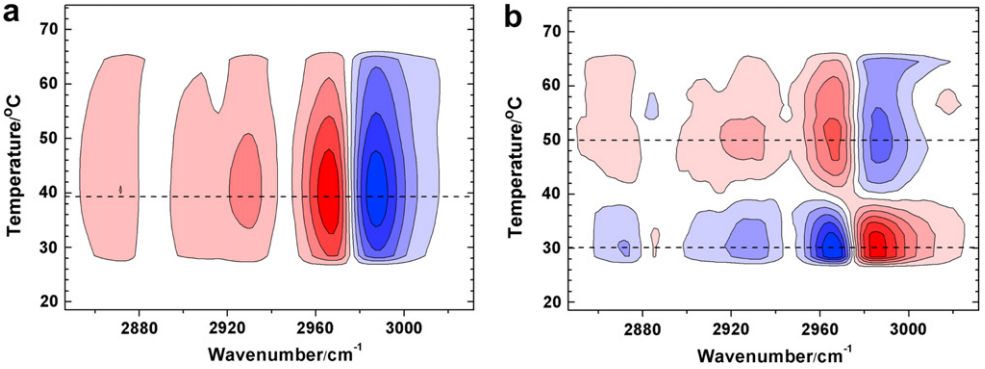

Fig. 5. 2D synchronous (a) and asynchronous (b) spectra of PCMW performed in the temperature range 18.5–70.5 °C in the regions (3030–2850 cm^{-1}) of NIPPA 40 wt% D_2O solution. Red colors are defined as positive intensities, while blue colors as negative ones. (For interpretation of the references to colour in this figure legend, the reader is referred to the web version of this article.)

Table 3
Band assignments of NIPPA and PNIPAM aqueous solution according to conventional IR as well as 2DIR.

PNIPAM		NIPPA	
Wavenumber/cm^{-1}	Assignment	Wavenumber/cm^{-1}	Assignment
2989	Hydrated $\nu_{as}(CH_3)$	2987	Hydrated $\nu_{as}(CH_3)$
2969	Less hydrated $\nu_{as}(CH_3)$	2966	Less hydrated $\nu_{as}(CH_3)$
2927	$\nu_{as}(CH_2)$	2929	$\nu_{as}(CH_2)$
2871	$\nu_s(CH_3)$	2873	$\nu_s(CH_3)$
1652	C═O···D–N	1652	C═O···D–N
1627	C═O···D–O–D	1600	C═O···(D–O–D)$_n$ ($n > 1$)

So in NIPPA system it would take long time to complete dehydration process so that phase separation is very mild, as indicated by our DSC measurement. In contrast, PNIPAM system takes less time completing and reaching stable level. Besides, two systems have different transition points, and transition temperature of 40 wt% NIPPA/D_2O solution is higher than that of 40 wt% PNIPAM/D_2O solution. So these results indicate that the reason of different features is induced by a great number of hydrophobic main chains in PNIPAM hindering from contact between water and amide groups, which aggravates occurrence of the phase separation.

3.4. 2DIR analysis for NIPPA systems

Based on above analysis and results, the different features of phase separation in NIPPA/D_2O and PNIPAM/D_2O solution have been discussed. To further compare these processes, we employ two-dimensional correlation analysis to explore the micro-dynamics mechanism of the phase transitions.

In 2D correlation analysis, two types of correlation maps (synchronous and asynchronous spectra) are obtained from a series of dynamic spectra, which are both characterized by two independent wavenumber axes (ν_1, ν_2) and a correlation intensity axis. In this paper, the red-colored and blue-colored areas in the 2DIR correlation contour maps represent positive and negative peaks, respectively. Synchronous spectra (marked it as Φ) is symmetric with respect to the diagonal line in the correlation map, while the asynchronous spectra (marked it as Ψ) is asymmetric with respect to the diagonal line in the correlation map Hence, combined with synchronous and asynchronous spectra, some useful information about the temporal sequence of events can be obtained according to Noda's rule [27,28] – that is, when $\Phi(\nu_1, \nu_2) > 0$, $\Psi(\nu_1, \nu_2) > 0$ or $\Phi(\nu_1, \nu_2) < 0$, $\Psi(\nu_1, \nu_2) < 0$, band ν_1 will vary prior to band ν_2. If $\Phi(\nu_1, \nu_2) > 0$, $\Psi(\nu_1, \nu_2) < 0$ or $\Phi(\nu_1, \nu_2) < 0$, $\Psi(\nu_1, \nu_2) > 0$, band ν_1 will vary after ν_2 under the environmental perturbation.

For the convenience of discussion, detailed band assignments in –CH and C═O regions according to conventional IR as well as 2DIR have been listed in Table 3. The synchronous and asynchronous maps for the heating process of the 40 wt% NIPPA/D_2O solution in the 3060–2850 cm^{-1} region are shown in Fig. 6. In the synchronous map (Fig. 6(a)), two strong autopeaks develop at 2987, 2966, 2929 and 2873 cm^{-1}. The first two autopeaks can been seen directly in Fig. 6(a), which points out the significant change of these two peaks as temperature rises, but the last two autopeaks are only detected from the slice spectra at the diagonal line because the intensities change is very weak in these regions. Besides, three negative crosspeaks and two positive crosspeaks can be observed in off-diagonal region. Those negative crosspeaks centered at (2987, 2966); (2987, 2929); (2987, 2873) cm^{-1} indicate that intensity variations of the above 2987 and 2966, 2929, 2873 cm^{-1} are taking place in the opposite direction. And another two positive crosspeaks ((2966, 2929); (2966, 2873) cm^{-1}) show intensity variations of 2966, 2929 and 2873 cm^{-1} bands are all taking place in the same direction.

On the other hand, the asynchronous 2DIR correlation spectra are shown in Fig. 6(b). Based on the rule put forward by Noda, the symbols of (2987, 2966); (2987, 2929); (2987, 2873) cm^{-1} are both negative in the synchronous and asynchronous maps. This reveals that the intensity of 2987 cm^{-1} band varies prior to those of 2966, 2929 and 2873 cm^{-1} bands when temperature is heating. Otherwise, the symbols of (2966, 2929); (2966, 2873) cm^{-1} are both positive in synchronous and asynchronous maps, which express the intensity of 2966 cm^{-1} band varies prior to those of 2929 and 2873 cm^{-1} bands under temperature-induced perturbation. So we can finally conclude changing sequence of four bands depicted as 2987 > 2966 > 2929, 2873 cm^{-1} (the symbol of ">" means change prior to).

In view of this sequence, the 2987 cm^{-1} peak of $\nu_{as}(CH_3)$ surrounded by many deuterated water molecules first decrease, and then becomes the less hydrated $\nu_{as}(CH_3)$ (2966 cm^{-1}). Those methyl groups rapidly give up large numbers of D_2O molecules as temperature rises to near LSCT so that the intensities of less hydrated $\nu_{as}(CH_3)$ increase quickly.

Except for the above discussion on C–H region, we also pay attention to Amide I region which is sensitive to conformation and secondary structures [31]. The synchronous and asynchronous spectra in amide I region are shown in Fig. 7. In the synchronous spectrum (Fig. 7(a)), two strong autopeaks at 1652 and 1600 cm^{-1},

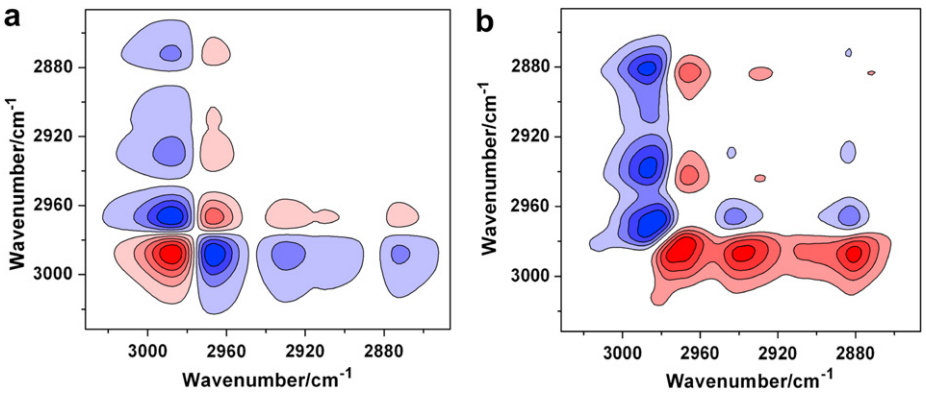

Fig. 6. The synchronous (a) and asynchronous (b) maps of the NIPPA 40 wt% D_2O solution in the region of 3030–2850 cm^{-1} representing the heating process.

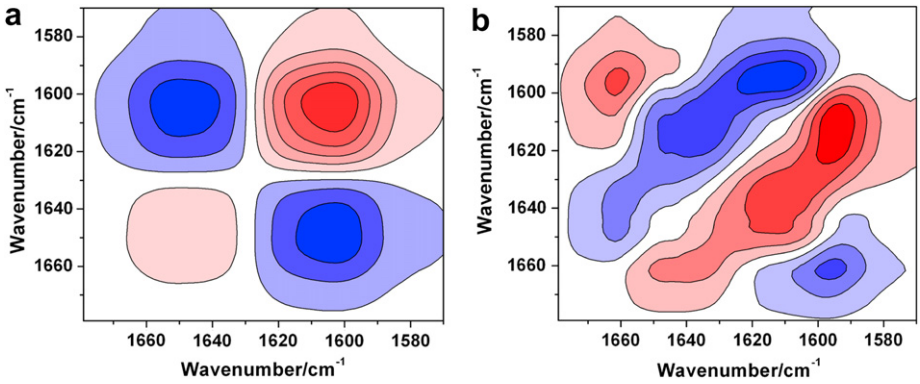

Fig. 7. The synchronous (a) and asynchronous (b) maps of the NIPPA 40 wt% D_2O solution in the region of 1680–1570 cm^{-1} representing the heating process.

and a negative crosspeak at (1652, 1600) cm^{-1} can be seen obviously. The two autopeaks are respectively attributed to the C═O···D–N and C═O···D–O–D hydrogen bonds of carbonyl stretching vibration. It is noticeable that the band of C═O···D–O–D (1600 cm^{-1}) in NIPPA system is 27 cm^{-1} lower than compared to that of PNIPAM (1627 cm^{-1}), which reveals that strength of the bond between C and O atoms is weakened and it can be characterized by magnitude of force constant (k) – $k_{(C=O\ in\ NIPPA)}$ = 1035.0 N/m; $k_{(C=O\ in\ PNIPAM)}$ = 1070.2 N/m.

$$\text{wavenumber}(cm^{-1})\cdot h(Js)\cdot c(m/s)\cdot 100(cm/m) = h\cdot(k/\mu)^{1/2}/2\pi$$

h: Planck's constant, c: the velocity of light in vacuum, k: the force constant (N/m), μ: $m_c m_o/(m_c + m_o)$, where m_c and m_o are masses (kg) of the two nuclei.

The more D atoms of D_2O share with the lone pair electrons of O atoms in carbonyl, the strength of carbonyl band becomes weaker. Therefore, we consider that carbonyls without hydrophobic polymer chains should be free to interact with more water molecules below LSCT and this carbonyl of multiple hydrogen bonds could be re-depicted as C═O···$(D–O–D)_n$ ($n > 1$) [5,32] (it is hard to determine the accurate number of water molecules H-bonding with carbonyl, so we take 'n' as subscript). Besides, the negative crosspeak (1652, 1600) cm^{-1} indicates that the band of C═O···$(D–O–D)_n$ is increasing while the band of C═O···D–N is decreasing during heating according to Noda's rule. Furthermore, because Φ(1652, 1600) cm^{-1} is negative and Ψ(1652, 1600) cm^{-1} is positive, we can infer that the change of the C═O···$(D–O–D)_n$ is prior to that of C═O···D–N when temperature rises. It means the hydrogen bonds of C═O···$(D–O–D)_n$ firstly consume and then the new hydrogen bonds of C═O···D–N form. Meanwhile, it will take longer time to complete the dissociation of C═O···$(D–O–D)_n$ and hydrogen bonds bridges, because carbonyls of NIPPA interact with more water below LSCT. That's the reason why the phase transition of NIPPA aqueous solution takes much more time than that of PNIPAM.

The analysis of the synchronous and asynchronous spectra which correlated amide I region with C–H region can help to supply the valuable complement for the whole phase separation process of NIPPA. In Fig. 8, several crosspeaks can be observed in the synchronous and asynchronous spectra, thus we can find the change sequence of different groups: 1600, 1652 > 2987, 2966, 2929, 2873 cm^{-1}, which means two types of carbonyl hydrogen bonds are both sensitive to temperature response and alter faster than all the C–H bands.

Based on the above these sequences which reveal the successive thermal sensitivity of different groups, it provides us important information on micro-mechanism of phase separation in NIPPA aqueous solution. In summary, the change sequence of all the bands can be found as follows: 1600 > 1652 > 2987 > 2966 > 2929, 2873 cm^{-1}. At first, the strong hydrogen bonds of C═O···$(D–O–D)_n$ linked with each other start to dissociate and form a new kind of hydrogen bonds (C═O···D–N) which stabilize the aggregation of NIPPA molecules, and then $–CH_3$ groups give up the surrounding water molecules and hinder water from interacting

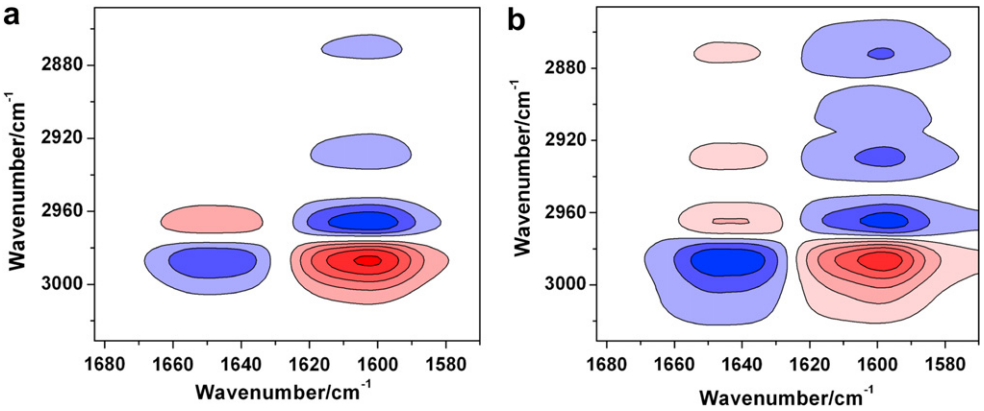

Fig. 8. The synchronous (a) and asynchronous (b) maps of the NIPPA 40 wt% D_2O solution in the region of 1683–1570 cm^{-1} and 3031–2846 cm^{-1} during the heating process.

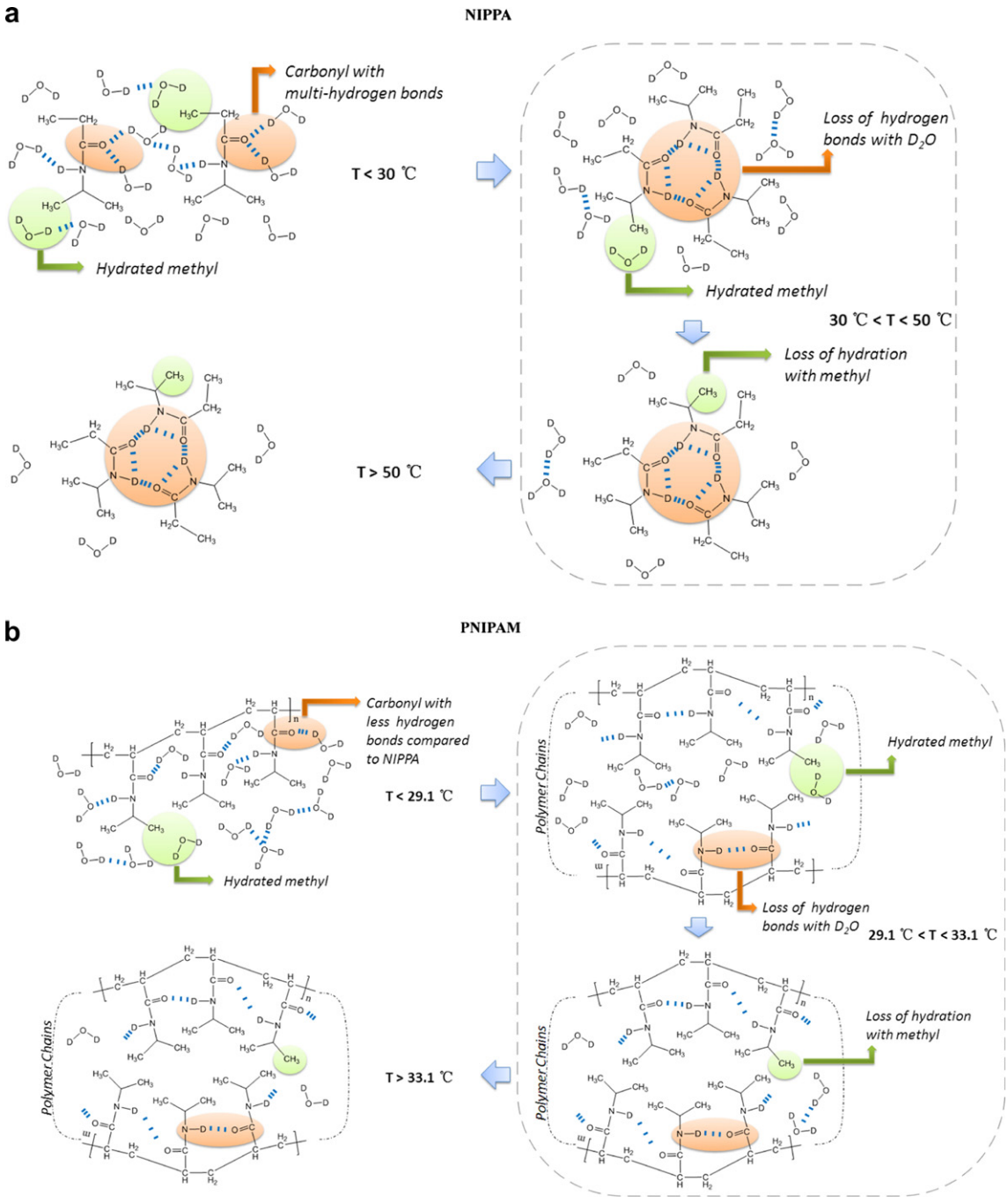

Scheme 2. Mechanism of temperature-induced phase transition of concentrated aqueous solutions of PNIPAM and NIPPA.

with amide groups. This explanation is illustrated clearly in Scheme 2(a). Because it's rather difficult to determine the number of the aggregation of NIPPA molecules, we have to draw an approximate figure to show the process of phase transition. Besides, this aggregation of NIPPA molecules is not as big as globular state of PNIPAM which has long polymer chain so that the phase separation of NIPPA system can't be found in visual observation.

3.5. 2DIR analysis for PNIPAM systems

For PNIPAM, we obtain some similar information of the whole phase separation process like NIPPA system. In synchronous and asynchronous spectra of amide I (Fig. 9(a, d)), C–H regions (Fig. 9(b, e)) and C–H/amide I cross-correlated regions (Fig. 9(c, f)), the sequence of all bands based on 2D analysis could be described as 1627 > 1652 > 2989 > 2969 > 2927 > 2871 cm^{-1}, which is summarized that when temperature rises, amide groups in side chains firstly give up those water molecules of C═O···D–O–D, and form the new hydrogen bonds of C═O···D–N so that polymer chains start to aggregate together. Then $–CH_3$ groups in side chains dehydrate with surrounding water and followed by $–CH_2–$ in main chain. Finally, PNIPAM aqueous solution completes the coil-to-globule transition at LSCT. This micro-mechanism can be depicted in Scheme 2(b).

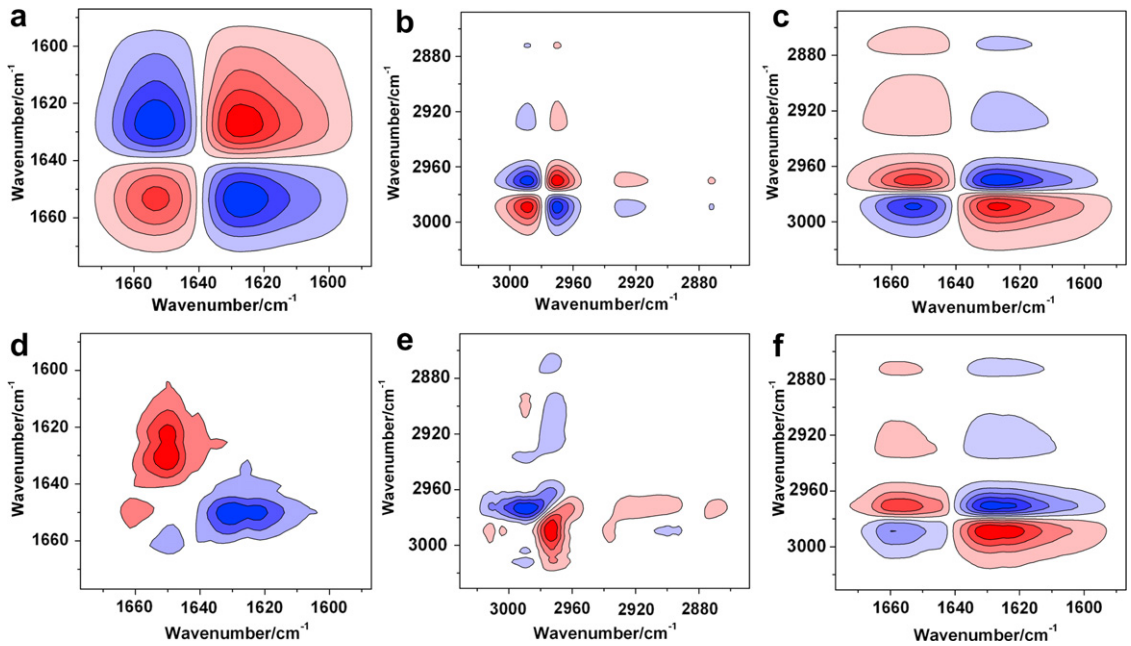

Fig. 9. The synchronous (a), (b), (c) and asynchronous (d), (e), (f) maps of the PNIPAM 40 wt% D_2O solution in the region of amide I, C–H regions and C–H/amide I cross-correlated regions during the heating process.

4. Conclusion

In the paper, a newly developed technique (PCMW) was employed to confirm the behavior of phase transition in PNIPAM and NIPPA aqueous solutions. In view of PCMW information based on spectral changes in $\nu_{as}(CH_3)$ region, we can discover the intensities change is not linear but "anti-S-shaped" and "S-shaped" in NIPPA aqueous solution which is the same as PNIPAM system. However, several different thermo-features have been measured. The transition point of NIPPA aqueous solution is at about 39 °C and the rapid dehydrated process takes place between 30 and 50 °C while the PNIPAM system just has narrow temperature range (29.1–33.1 °C) and LCST is at 31.2 °C, which can be testified by DSC measurement.

Although the transition points and the temperature ranges of phase separation are quite different in NIPPA and PNIPAM systems, their microcosmic mechanisms are almost the same. We utilize 2DIR method to obtain the changing sequence of four bands followed as: the hydrogen bonds of C═O···(D–O–D)$_m$ ($m \geq 1$) first break → more hydrogen bonds of C═O···D–N increases →hydrated –CH_3 groups give up those water molecules → less hydrated –CH_3 groups increase → –CH_2 groups finally dehydrate. Thus, it can deduce hydrogen bonds and dehydration are both the driving forces of phase transition, and that the sensitivity and changing sequence of different groups are not affected by the presence of main chains. But those polymer chains are related to the size of the globular state above LCST because the aggregation of polymer chains is big enough that we can easily observe the phenomenon of phase separation by our eyes instead of microscope. Without the interference of hydrophobic main chains, the carbonyls of NIPPA have interacted with more water than those of PNIPAM, so the phase transition of NIPPA aqueous solution takes place in the slower and milder process, which helps us to further explain the micro-dynamics mechanism of the phase separation.

Acknowledgement

We gratefully acknowledge the financial support of National Science Foundation of China (NSFC) (No. 20934002, 20774022), the National Basic Research Program of China (No. 2005CB623800, 2009CB930000) and Open Project of State Key Laboratory of Supramolecular Structure and Materials (SKLSSM200717).

References

[1] Cheng H, Shen L, Wu C. Macromolecules 2006;39:2325.
[2] Katsumoto Y, Tanaka T, Sato H, Ozaki Y. J Phys Chem A 2002;106:3429.
[3] Katsumoto Y, Tanaka T, Ozaki Y. Macromol Symp 2004;205:209.
[4] Ono Y, Shikata T. J Am Chem Soc 2006;128:10030.
[5] Ono Y, Shikata T. J Phys Chem B 2007;111:1511.
[6] Starovoytova L, Spevacek J, Ilavsky M. Polymer 2005;46:677.
[7] Starovoytova L, Spevacek J. Polymer 2006;47:7329.
[8] Starovoytova L, Spevacek J, Trchova M. Eur Polym J 2007;43:5001.
[9] Kano M, Kokufuta E. Langmuir 2009;25:8649.
[10] Sanchez MS, Hanykova L, Ilavsky M, Pradas MM. Polymer 2004;45:4087.
[11] Cho EC, Lee J, Cho K. Macromolecules 2003;36:9929.
[12] Nuopponen M, Ojala J, Tenhu H. Polymer 2004;45:3643.
[13] Meersman F, Wang J, Wu YQ, Heremans K. Macromolecules 2005;38:8923.
[14] Sun B, Lin Y, Wu P, Siesler HW. Macromolecules 2008;41:1512.
[15] Lin SY, Chen KS, Run-Chu L. Polymer 1999;40:6307.
[16] Percot A, Zhu XX, Lafleur M. J Polym Sci Part B: Polym Phys 2000;38:907.
[17] Maeda Y, Nakamura T, Ikeda I. Macromolecules 2001;34:1391.
[18] Maeda Y, Nakamura T, Ikeda I. Macromolecules 2001;34:8246.
[19] Maeda Y, Yamamoto H, Ikeda I. Macromolecules 2003;36:5055.
[20] Schmidt P, Dybal J, Trchova M. Vib Spectrosc 2006;42:278.
[21] Dybal J, Trchova M, Schmidt P. Vib Spectrosc 2009;51:44.
[22] Jung SC, Bae YC. Polymer 2009;50:4957.
[23] Geukens B, Meersman F, Nies E. J Phys Chem B 2008;112:4474.
[24] Thomas M, Richardson HH. Vib Spectrosc 2000;24:137.
[25] Morita S, Shinzawa H, Noda I, Ozaki Y. Appl Spectrosc 2006;60:398.
[26] Unger M, Morita S, Sato H, Ozaki Y, Siesler HW. Appl Spectrosc 2009;63:1027.
[27] Noda I. Appl Spectrosc 1993;47:1329.
[28] Noda I, Dowrey AE, Marcott C, Story GM, Ozaki Y. Appl Spectrosc 2000;54:236A.
[29] Sun BJ, Lin YA, Wu PY. Appl Spectrosc 2007;61:765.
[30] Maeda Y, Higuchi T, Ikeda I. Langmuir 2000;16:7503.
[31] Ganim Z, Chung HS, Smith AW, Deflores LP, Jones KC, Tokmakoff A. Acc Chem Res 2008;41:432.
[32] Maeda Y, Sakamoto J, Wang SY, Mizuno Y. J Phys Chem B 2009;113:12456.